Acta Crystallographica Section F
Structural Biology Communications
ISSN 2053-230X

The structure of rice weevil pectin methylesterase

David C. Teller,[a,b] Craig A. Behnke,[a]‡ Kirk Pappan,[c]§ Zicheng Shen,[c]¶ John C. Reese,[d] Gerald R. Reeck[c] and Ronald E. Stenkamp[a,b,e]*

[a]Department of Biochemistry, University of Washington, Box 357430, Seattle, WA 98195-7430, USA, [b]Biomolecular Structure Center, University of Washington, Box 357742, Seattle, WA 98195-7742, USA, [c]Department of Biochemistry and Molecular Biophysics, Kansas State University, Manhattan, KS 66506, USA, [d]Department of Entomology, Kansas State University, Manhattan, KS 66506, USA, and [e]Department of Biological Structure, University of Washington, Box 357420, Seattle, WA 98195-7420, USA

‡ Current address: Sapphire Energy Inc., San Diego, CA 92121, USA.
§ Current address: Metabolon Inc., Durham, NC 27713, USA.
¶ Current address: Institute of Insect Science, Zhejiang University, Hangzhou 310058, People's Republic of China.

Correspondence e-mail: stenkamp@u.washington.edu

Received 5 August 2014
Accepted 11 September 2014

PDB reference: pectin methylesterase, 4pmh

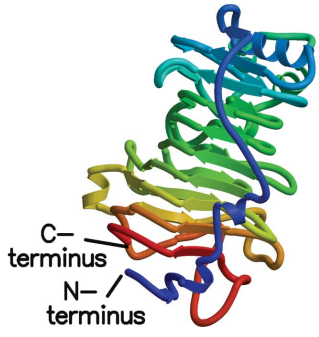

Rice weevils (*Sitophilus oryzae*) use a pectin methylesterase (EC 3.1.1.11), along with other enzymes, to digest cell walls in cereal grains. The enzyme is a right-handed β-helix protein, but is circularly permuted relative to plant and bacterial pectin methylesterases, as shown by the crystal structure determination reported here. This is the first structure of an animal pectin methylesterase. Diffraction data were collected to 1.8 Å resolution some time ago for this crystal form, but structure solution required the use of molecular-replacement techniques that have been developed and similar structures that have been deposited in the last 15 years. Comparison of the structure of the rice weevil pectin methylesterase with that from *Dickeya dandantii* (formerly *Erwinia chrysanthemi*) indicates that the reaction mechanisms are the same for the insect, plant and bacterial pectin methylesterases. The similarity of the structure of the rice weevil enzyme to the *Escherichia coli* lipoprotein YbhC suggests that the evolutionary origin of the rice weevil enzyme was a bacterial lipoprotein, the gene for which was transferred to a primitive ancestor of modern weevils and other Curculionidae. Structural comparison of the rice weevil pectin methylesterase with plant and bacterial enzymes demonstrates that the rice weevil protein is circularly permuted relative to the plant and bacterial molecules.

1. Introduction

Plant cell walls consist of an organized arrangement of complex polysaccharides and proteins which serve as cell structure and plant defense. Nutritionally, plants are a rich source of food if an organism can disrupt and digest these plant products. Following the reports of Shen and coworkers (Shen *et al.*, 1996, 1999, 2003, 2005), it has become clear that the family of Curculionoidae beetles and weevils uses cellulolytic and pectolytic enzymes to aid the invasion and digestion of cereal grains, especially rice and wheat. Initially, it was thought that these enzymes may have been present in the endo-symbiotic organisms in the gut of the rice weevils (*Sitophilus oryzae*), but the study by Shen *et al.* (2005) demonstrated that the pectin methylesterase (PME) was encoded by the rice weevil genome. Amino-acid sequence comparisons suggest that similar enzymatic functions operate in the interactions between other Curculionoidae beetles and plants (see Pauchet *et al.*, 2010).

Galacturonase and pectate lyase cannot act enzymatically on pectin, but require de-esterification of pectin to pectate in order to digest the polymer. Therefore, pectin methylesterase is central to an insect's ability to use pectin and pectate as a food source. Additionally, the hydrolysis of these compounds allows the insect to access the cell contents as a source of further nutrition. The rice weevil is an abundant source of PME, which allowed its isolation, purification and characterization (Shen *et al.*, 1999, 2005).

We initiated our structural studies of rice weevil PME (RW PME) 15 years ago, but we were unable to solve the crystal structure with the software and template structures available at the time. Recently, we succeeded in solving the structure using the *BALBES* molecular-replacement server (Long *et al.*, 2008) and the automatic electron-density fitting program *ARP/wARP* (Langer *et al.*, 2008). Also contributing to the success of this approach are the similar structures that have been solved and deposited recently (Jenkins *et al.*, 2001; Johansson *et al.*, 2002; Di Matteo *et al.*, 2005; Eklöf *et al.*, 2009; Boraston & Abbott, 2012).

2. Materials and methods

2.1. Protein expression, crystallization and diffraction data collection

RW PME was purified as described previously (Shen *et al.*, 1999, 2005). Crystals of RW PME were obtained from hanging-drop vapor-diffusion experiments, but the details of the conditions have been lost owing to a hacked computer. Needles appeared shortly after the crystallization trials were set up, but it took a year for the crystals to assume a useable form. Heavy-atom soaks were performed, but the resulting crystals were non-isomorphous and diffracted poorly. Since only 4 mg of protein was available, all trial conditions were severely limited in scope. The space group of the crystals is $C222_1$, with unit-cell parameters a = 37.43, b = 73.94, c = 204.90 Å and one RW PME molecule in the asymmetric unit. Diffraction data for RW PME were collected at the Structural Biology Center at the Advanced Photon Source at 100 K. Data sets were processed using *DENZO* and *SCALEPACK* (Otwinowski & Minor, 1997). A summary of the statistics is presented in Table 1.

2.2. Structure solution and refinement

The structure of RW PME was solved with *BALBES* (Long *et al.*, 2008) and *ARP*/*wARP* (Langer *et al.*, 2008). The amino-acid sequence used in the first structure determination had been truncated, but the initial model produced by *BALBES* and *ARP*/*wARP* and refined using *REFMAC*5 (Murshudov *et al.*, 2011) yielded an R value of 0.20, indicating a correct solution. The resulting electron-density maps could be easily fitted with most of the residues missing in the input sequence file. A second run of *BALBES* and *ARP*/*wARP* with a corrected sequence produced a model lacking only seven residues. These were located in subsequent electron-density maps. The complete model was then refined using *REFMAC*5 in the *CCP*4 program suite (Winn *et al.*, 2011). 5% of the reflections were reserved for calculation of $R_{\rm free}$ (Brünger, 1992).

XtalView (McRee, 1999) and *Coot* (Emsley *et al.*, 2010) were used to view $\sigma_{\rm A}$-weighted $|F_{\rm o}| - |F_{\rm c}|$ and $2|F_{\rm o}| - |F_{\rm c}|$ electron-density maps (Read, 1986) and to manipulate the molecular models. The structural models were evaluated during and after refinement using *MolProbity* (Chen *et al.*, 2010) and *ADIT* (Berman *et al.*, 2000). Figures were generated using *MolScript* (Kraulis, 1991) and *Raster*3*D* (Merritt & Bacon, 1997).

The final model for RW PME contains residues 1–366 and 299 water molecules. Refinement statistics for the structure are given in Table 1. Coordinates and structure factors for RW PME have been deposited in the Protein Data Bank (with code 4pmh).

Table 1
Data-collection and refinement statistics.

Values in parentheses are for the inner/outer shell.

Diffraction data statistics	
Unit-cell parameters (Å)	a = 37.43, b = 73.94, c = 204.90
Space group	$C222_1$
Low-resolution limit (Å)	99.0 (99.0/1.85)
High-resolution limit (Å)	1.79 (3.85/1.79)
$R_{\rm merge}$	0.085 (0.066/0.296)
No. of unique reflections	23540 (2896/1357)
$\langle I\rangle/\langle\sigma(I)\rangle$	12.7 (21.0/2.2)
Completeness (%)	85.6 (98.1/50.7)
Multiplicity	3.5 (6.0/1.3)
Refinement statistics	
Resolution (Å)	102.5–1.79
No. of reflections, working set	21081
No. of reflections, test set	1203
$R_{\rm cryst}$, all data	0.176
$R_{\rm cryst}$, working set	0.173
$R_{\rm free}$, test set	0.226
Bond r.m.s. (restrained) (Å)	0.010
No. of protein atoms	2753
No. of solvent atoms	299
Ramachandran outliers as determined by *MolProbity* (%)	0.0
Ramachandran favored (%)	96.2
PDB code	4pmh

Sequence alignments were constructed with the *Clustal Omega* web server (http://www.ebi.ac.uk/Tools/msa/clustalo/) using default parameters (Sievers *et al.*, 2011).

The sequences were gathered using the sequence published by Shen *et al.* (2005) (AAW28928.1) and those for RW PME deposited by Pauchet *et al.* (2010). The sequence ADU33259.1 of Pauchet *et al.* (2010) is 98% identical to that of Shen *et al.* (2005). There were eight differences between these sequences. For seven of the eight differences the ADU33259.1 sequence fitted the electron density better than the AAW28928.1 sequence and therefore the former was used; the exception was position 61, where we have used the Ala from AAW28928.1. For our numbering of the sequence, we have used the start at DQTA as suggested by Shen *et al.* (2005) and this matches the electron density.

For the structural alignment of the carbohydrate esterase family (CE8), we used a locally written program which adaptively fits the translation/rotation matrix of a query to target proteins with sequence numbers increasing and within a given window and a specified tolerance based on a preliminary sequence alignment. Using

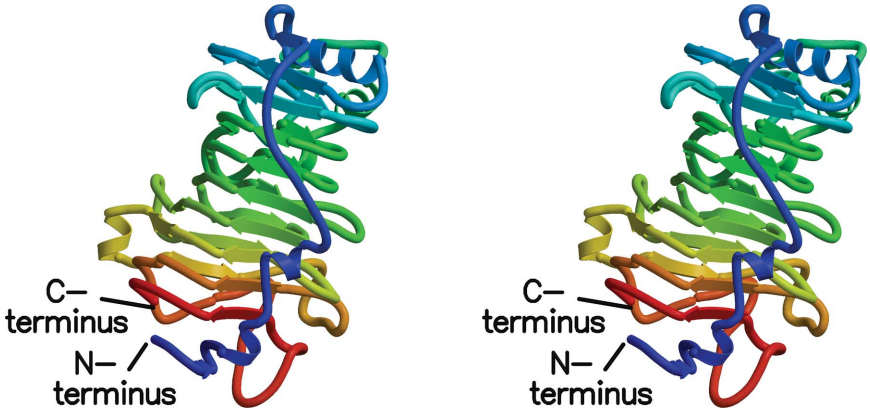

Figure 1
Stereo diagram of rice weevil pectin methylesterase. The β-strands of the right-handed β-helix are denoted by arrows. The coils show the few α-helices in the structure. Coloring is from blue at the N-terminus to red at the C-terminus. Note the close proximity of the N- and C-termini.

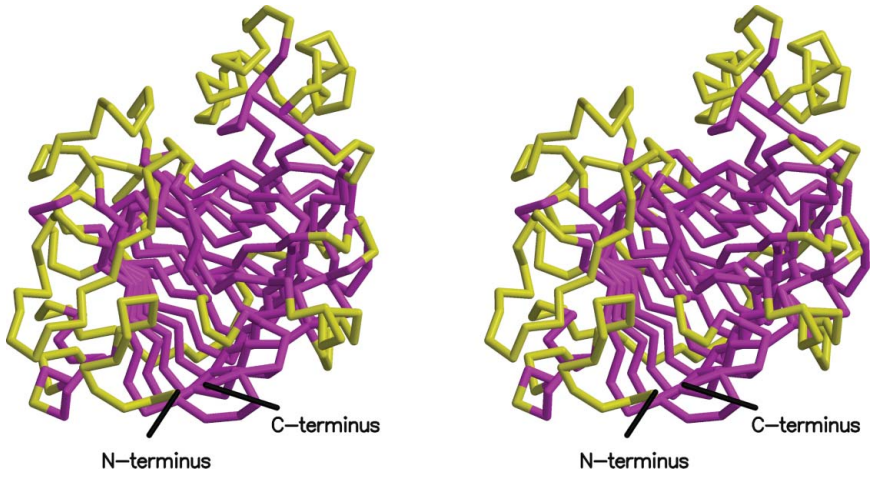

Figure 2
Stereo diagram of RW PME with the structural core found in six superposed structures (Table 2) shown in magenta. The residues making up the core are consecutive runs of residues with C^{α} atoms that superpose to within 3 Å.

this program, all of the PMEs in the Protein Data Bank were superposed on the RW PME coordinates, as was the YbhC lipoprotein of *Escherichia coli* (Eklöf *et al.*, 2009).

Locally written programs were also used to demonstrate the structural similarity of the N-terminal region of RW PME and the C-terminal regions of plant and bacterial PMEs.

3. Results

The structures of all of the proteins downloaded from the Protein Data Bank under the name pectin methylesterase are similar right-handed β-helices (Fig. 1). A structural characteristic of β-helix proteins is the stacking of hydrophobic and aromatic side chains on the inside and outside of the β-helix (Jenkins & Pickersgill, 2001). Similar packings are seen in RM PME, where the arrangement of β-strands in the overall helix ensures that the side chains will be stacked in a slight twist along the direction of the helical axis.

A sequence alignment of the PMEs (and the YbhC lipoprotein from *E. coli*; Eklöf *et al.*, 2009; Supplementary Fig. S1[1]) and a three-dimensional structure alignment generated using our adaptive superposition program (Table 2) provide a basis for comparing the proteins. From the results tabulated in the table, it is unclear whether RW PME is closer to the bacterial or plant PMEs in structure. It is clear that the two plant enzymes are similar to each other, as are the two bacterial PMEs.

A common structural core for the six proteins is made up of runs of consecutive residues that superpose to within 3 Å (see Fig. 2). Despite the remarkable superposition of the structures, the N-terminal region of RW PME is significantly longer than in the other enzymes and the C-terminal region is shorter. Noteworthy is the fact that the plant and bacterial enzymes have the N- and C-terminal residues rather close together. This is even more extreme in the case of RW PME as these two residues are only 5.8 Å apart at the C^{α} atoms. When all six proteins are superposed, one sees that the N-terminal region of RW PME aligns with the C-terminal regions of the plant and bacterial enzymes. This is shown in Fig. 3 for the *Dickeya dadantii* (formerly *Erwinia chrysanthemi*) enzyme compared with the RW PME. This circular permutation is discussed more fully below.

[1] Supporting information has been deposited in the IUCr electronic archive (Reference: DW5113).

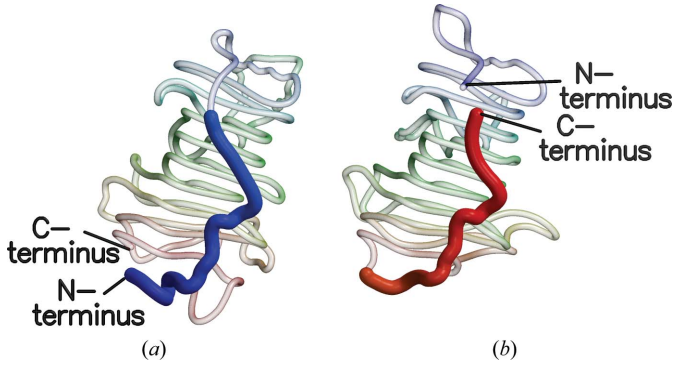

Figure 3
These diagrams of (*a*) RW PME and (*b*) *D. dadantii* PME demonstrate the circular permutation of the protein structures relative to one another. The N-terminal region of RW PME is extended, but when the structures are superposed it conforms to the C-terminal region of the bacterial and plant PMEs.

Table 2
Distances (Å) among PMEs measured *via* r.m.s. fit of C^{α} atoms using our alignment program.

The lower number is the number of distinct residues which were found to fit within 3 Å in the best-fit procedure. Our program adaptively fits the query and target proteins with the sequence numbers increasing within the given window (90 residues in this case) and within the specified tolerance (3 Å in this case). 4pmh is RW PME, 3grh is the YbhC lipoprotein from *E. coli* (Eklöf *et al.*, 2009), 1gq8 is the PME from carrot (*Daucus carota*; Johansson *et al.*, 2002), 1xg2 is the PME from tomato (*Solanum lycopersicum*; Di Matteo *et al.*, 2005), 1qjv is the PME from *D. dadantii* (Jenkins *et al.*, 2001) and 3uw0 is the PME from *Yersinia enterocolitica* (Boraston & Abbott, 2012).

	3grh	1gq8 (chain *A*)	1xg2 (chain *A*)	1qjv (chain *A*)	3uw0
4pmh (chain *A*)	1.033	1.083	1.000	1.017	1.075
	343	223	224	245	229
3grh (chain *A*)		1.063	1.036	1.153	1.086
		238	227	255	238
1gq8 (chain *A*)			0.702	1.138	1.161
			313	242	221
1xg2 (chain *A*)				1.137	1.178
				260	248
1qjv (chain *A*)					0.753
					315

For the most part, the protein chain of RW PME tracks the other PMEs fairly closely. Between residues 113 and 142 there is an extra loop of two helices which is not present in the other enzymes but is present in the lipoprotein YbhC. This loop points away from the active-site groove, so it should not interfere with the enzyme activity.

In the region of RW PME residues 171–176 the bacterial enzymes have a longer loop than the plant or RW PME enzymes. At the RW PME loop from residues 206 to 212 the lipoprotein YbhC has a longer loop (loop 2 in Fig. 2 of Eklöf *et al.*, 2009), which is said to prevent pectin methylesterase activity. In the RW PME this seven-residue loop is longer than the plant and bacterial enzymes but protrudes into the active-site groove less than the 15-residue loop of YbhC. Indeed, the 15-residue loop of YbhC collides with the docked hexagalacturonic acid substrate (Fries *et al.*, 2007), but the loop of RW PME does not. Unlike the YbhC protein, the RW PME is an active enzyme (Shen *et al.*, 1999).

The shape of the loop of RW PME from residues 295 to 307 differs from that in the bacterial enzymes. The structure of the loop from residues 339 to 353 is also rather different from the rest of the plant and bacterial enzymes, but from residue 353 to the C-terminus at 366 the structures of all of the enzymes superpose well.

4. Discussion

There are two more observations to make about the comparison of the structures of RW PME and the *E. coli* lipoprotein YbhC. Firstly, the structure of YbhC is more similar to RW PME than are the plant or bacterial enzymes. In the structural superposition of YbhC on RW PME, the root-mean-square fit of the C^{α} atoms is 1.033 Å for 343 residues, which is almost the entire length of the RW PME enzyme (94% of the 366 residues; see Table 2).

Secondly, the enzymatic function of the YbhC lipoprotein remains unknown (Eklöf *et al.*, 2009). It is not likely to be a PME, because an Asn residue in the YbhC lipoprotein superposes on a catalytic Asp in the PMEs (Table 3). The rice weevil has a putative protein, ADU33263.1, which similarly has Asn rather than Asp at the active center. The Asp at this position acts as a general acid–base in the reaction mechanism (Fries *et al.*, 2007). Sequence alignment of the YbhC protein compared with the RW ADU33263.1 protein indicates that the loop that blocks pectin binding in YbhC (residues 229–243) is very much truncated in the RW homolog.

Fries *et al.* (2007) determined the structures of seven PMEs, each of which had a hexasaccharide of varying methylation or pH of crystallization. We aligned these proteins with RW PME and then asked which residues of RW PME are in contact with the hexasaccharide ligand (Figs. 4 and 5, Table 3). The residues of RW PME in contact with these hexasaccharide ligands are completely compatible with those found for *D. dadantii* PME, and the enzyme mechanism proposed by Fries *et al.* (2007) can be assumed to apply directly to RW PME.

Table 3
Active-site residues in superposed CE8 proteins.

Note: residue numbers are those in the PDB files. 3grh is a lipoprotein with no PME activity.

4pmh	Gln199	Asp200	Asp226
3grh	Gln223	Asn224	Asp257
1gq8	Gln135	Asp136	Asp157
1qjv	Gln131	Asp132	Asp153
1xg2	Gln177	Asp178	Asp199
3uw0	Gln176	Asp177	Asp199

The final issue to address in the comparison of these enzymes is the circular permutation of the sequences. Circular permutation of protein sequences is uncommon but does occur naturally (Lindqvist & Schneider, 1997). The permutations originate by either of two mechanisms: genetic or post-translational. The sequence of the lectin concanavalin A from jack bean is circularly permuted from that of favin (Cunningham *et al.*, 1979) and occurs post-translationally. In the case of RW PME, the circular permutation is genetic in origin as seen from the encoding RNA sequences of all of the RW PME proteins.

As a final note, we have aligned the available sequences of the other Curculionidae PMEs (from the pine beetle *Dendroctonus ponderosae* and the sugarcane weevil *Sphenophorus levis*) with the rice weevil PME sequences. All of these proteins have the extended N-terminal region and truncated C-terminal region, indicating that

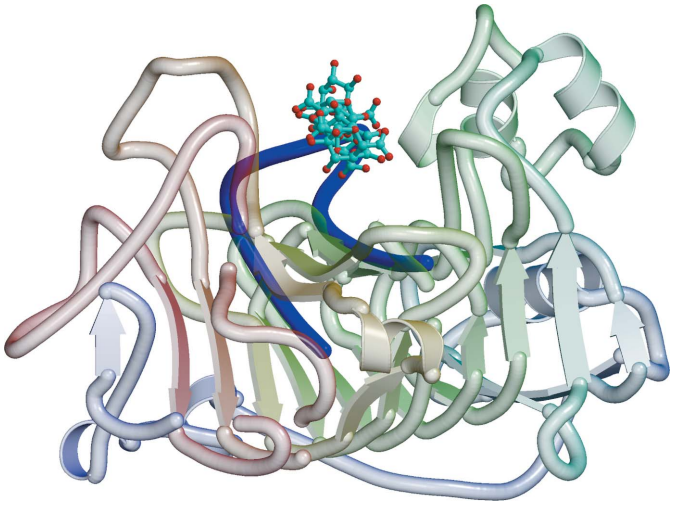

Figure 4
Model of the binding of the hexasaccharide V of Fries *et al.* (2007) in the active site of RW PME. The hexasaccharide is shown in ball-and-stick representation on a ribbon background of the protein. The loop from a superposed YbcH lipoprotein that would interfere with binding of the hexasaccharide is shown as a blue coil.

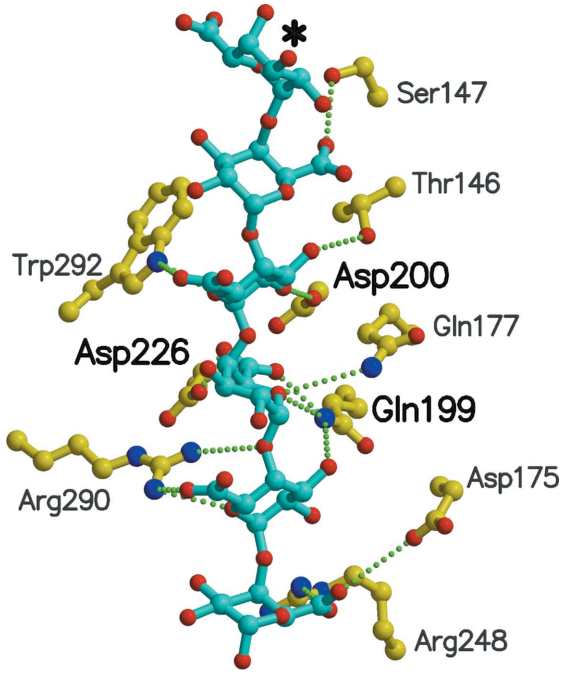

Figure 5
RW PME residues in contact with hexasaccharide V when its complex with YbhC (Fries *et al.*, 2007) is superposed onto RW PME. This hexasaccharide V simulates the product of the reaction since it consists of galacturonic acid residues. Bold labels denote residues involved in catalysis and transition-state stabilization. The asterisk denotes the reducing end of the hexasaccharide.

the circular permutation relative to the plant and bacterial enzymes is characteristic of this insect family.

5. Conclusions

The structure of RW PME has been determined using techniques of molecular replacement which were unavailable 15 years ago. The structures of the members of the CE8 protein family, while sharing a core structure, differ considerably in the loops and turns between the strands in the β-helix motif. Clearly, current molecular-replacement and model-building methods can deal with the differences between the bacterial and plant PMEs and the final structure of this enzyme.

Eklöf *et al.* (2009) investigated the phylogeny of the YbhC lipoprotein from *E. coli* and concluded that it occurred in a separate branch of the CE8 family. This is the protein which is most similar to RW PME and is similarly circularly permuted from the remainder of bacterial and plant enzymes.

Our efforts have determined the structure of the first PME from an animal source. Carbohydrate esterase family 8 (CE8) enzymes have to date only been found in the family Curculionideae, the family of true weevils and bark beetles (Pauchet *et al.*, 2010). Pauchet *et al.* (2010) identified sequences for five CE8 family pectolytic enzymes from rice weevil. Shen *et al.* (2005) determined the sequence of tissue-based PME, also from rice weevil. Their sequence is 98% identical to one of those deposited by Pauchet *et al.* (2010). The sequences differ in several positions, and based on our electron-density map the structural model has a sequence that is a combination of those two.

Sequence alignments of all of the known beetle PMEs indicate they are circularly permuted relative to the bacterial and plant PMEs. The YbcH lipoprotein, while found in a bacterium, is not a PME. We speculate that all of the isozymes of PME in rice weevil have evolved from a bacterial lipoprotein similar to the *E. coli* YbhC protein after horizontal transfer of the bacterial gene to the genome of a predecessor to curculionids.

6. Related literature

The following reference is cited in the Supporting Information for this article: Kabsch & Sander (1983).

We thank the Structural Biology Center, Argonne National Laboratory for beamtime for data collection. Use of the Advanced Photon Source, an Office of Science User Facility operated for the US Department of Energy (DOE) Office of Science by Argonne National Laboratory, was supported by the US DOE under Contract No. DE-AC02-06CH11357. The research reported in this publication was partially supported by the National Institute of General Medical Sciences of the National Institutes of Health under Award No. T32GM008268. The content is solely the responsibility of the authors and does not necessarily represent the official views of the National Institutes of Health. Portions of this work were also supported by the Kansas Agricultural Experiment Station (contribution No. 15-027-J) and by grants from the National Science Foundation (MCB-9974805) and the National Research Initiative of the USDA Cooperative State Reseach, Education and Extension Service (grant No. 2001-35302-09978).

References

Berman, H. M., Westbrook, J., Feng, Z., Gilliland, G., Bhat, T. N., Weissig, H., Shindyalov, I. N. & Bourne, P. E. (2000). *Nucleic Acids Res.* **28**, 235–242.
Boraston, A. B. & Abbott, D. W. (2012). *Acta Cryst.* F**68**, 129–133.
Brünger, A. T. (1992). *Nature (London)*, **355**, 472–475.
Chen, V. B., Arendall, W. B., Headd, J. J., Keedy, D. A., Immormino, R. M., Kapral, G. J., Murray, L. W., Richardson, J. S. & Richardson, D. C. (2010). *Acta Cryst.* D**66**, 12–21.
Cunningham, B. A., Hemperly, J. J., Hopp, T. P. & Edelman, G. M. (1979). *Proc. Natl Acad. Sci. USA*, **76**, 3218–3222.
Di Matteo, A., Giovane, A., Raiola, A., Camardella, L., Bonivento, D., De Lorenzo, G., Cervone, F., Bellincampi, D. & Tsernoglou, D. (2005). *Plant Cell*, **17**, 849–858.
Eklöf, J. M., Tan, T.-C., Divne, C. & Brumer, H. (2009). *Proteins*, **76**, 1029–1036.
Emsley, P., Lohkamp, B., Scott, W. G. & Cowtan, K. (2010). *Acta Cryst.* D**66**, 486–501.
Fries, M., Ihrig, J., Brocklehurst, K., Shevchik, V. E. & Pickersgill, R. W. (2007). *EMBO J.* **26**, 3879–3887.
Jenkins, J., Mayans, O., Smith, D., Worboys, K. & Pickersgill, R. W. (2001). *J. Mol. Biol.* **305**, 951–960.
Jenkins, J. & Pickersgill, R. (2001). *Prog. Biophys. Mol. Biol.* **77**, 111–175.
Johansson, K., El-Ahmad, M., Friemann, R., Jörnvall, H., Markovic, O. & Eklund, H. (2002). *FEBS Lett.* **514**, 243–249.
Kabsch, W. & Sander, C. (1983). *Biopolymers*, **22**, 2577–2637.
Kraulis, P. J. (1991). *J. Appl. Cryst.* **24**, 946–950.
Langer, G., Cohen, S. X., Lamzin, V. S. & Perrakis, A. (2008). *Nature Protoc.* **3**, 1171–1179.
Lindqvist, Y. & Schneider, G. (1997). *Curr. Opin. Struct. Biol.* **7**, 422–427.
Long, F., Vagin, A. A., Young, P. & Murshudov, G. N. (2008). *Acta Cryst.* D**64**, 125–132.
McRee, D. E. (1999). *J. Struct. Biol.* **125**, 156–165.
Merritt, E. A. & Bacon, D. J. (1997). *Methods Enzymol.* **277**, 505–524.
Murshudov, G. N., Skubák, P., Lebedev, A. A., Pannu, N. S., Steiner, R. A., Nicholls, R. A., Winn, M. D., Long, F. & Vagin, A. A. (2011). *Acta Cryst.* D**67**, 355–367.
Otwinowski, Z. & Minor, W. (1997). *Methods Enzymol.* **276**, 307–326.
Pauchet, Y., Wilkinson, P., Chauhan, R. & ffrench-Constant, R. H. (2010). *PLoS One*, **5**, e15635.
Read, R. J. (1986). *Acta Cryst.* A**42**, 140–149.
Shen, Z. C., Denton, M., Mutti, N., Pappan, K., Kanost, M. R., Reese, J. C. & Reeck, G. R. (2003). *J. Insect Sci.* **3**, 1–9.
Shen, Z., Manning, G., Reese, J. C. & Reeck, G. R. (1999). *Insect Biochem. Mol. Biol.* **29**, 209–214.
Shen, Z., Pappan, K., Mutti, N. S., He, Q.-J., Denton, M., Zhang, Y., Kanost, M. R., Reese, J. C. & Reeck, G. R. (2005). *J. Insect Sci.* **5**, 21.
Shen, Z., Reese, J. C. & Reeck, G. R. (1996). *Insect Biochem. Mol. Biol.* **26**, 427–433.
Sievers, F., Wilm, A., Dineen, D., Gibson, T. J., Karplus, K., Li, W., Lopez, R., McWilliam, H., Remmert, M., Söding, J., Thompson, J. D. & Higgins, D. G. (2011). *Mol. Syst. Biol.* **7**, 539.
Winn, M. D. *et al.* (2011). *Acta Cryst.* D**67**, 235–242.